High-Q double-disk microcavities for cavity optomechanics

Xiaoshun Jiang[1,2], Qiang Lin[1], Jessie Rosenberg[1], Kerry Vahala[1], and Oskar Painter[1]

[1]*Department of Applied Physic, California Institute of Technology, Pasadena, California, 91125, USA*
[2] *State Key Laboratory of Modern Optical Instrumentation, Department of Optical Engineering, Zhejiang University, Hangzhou 310027, China*
**opainter@caltech.edu*

Abstract: We design a double-disk microcavity consisting of a pair of silica microdisks separated by a nanoscale gap region on a silicon chip for cavity optomechanics. We show that this type of photonic structure can provide a per-photon gradient force with a magnitude much larger than for scattering-force-based structures. Moreover, this device provides for nearly independent optimization of optical and mechanical properties. We present the processing details of fabricated devices.

OCIS codes: (200.4880) Optomechanics; (140.3945) Microcavities.

References and links

1. T. J. Kippenberg, and K. J. Vahala, "Cavity opto-mechanics," Opt. Express **15**(25), 17172–17205 (2007), http://www.opticsinfobase.org/oe/abstract.cfm?URI=oe-15-25-17172.
2. T. J. Kippenberg, and K. J. Vahala, "Cavity Optomechanics: Back-Action at the Mesoscale," Science **321**(5893), 1172–1176 (2008).
3. I. Favero, and K. Karrai, "Optomechanics of deformable optical cavities," Nat. Photonics **3**(4), 201–205 (2009).
4. T. Carmon, H. Rokhsari, L. Yang, T. J. Kippenberg, and K. J. Vahala, "Temporal Behavior of Radiation-Pressure-Induced Vibrations of an Optical Microcavity Phonon Mode," Phys. Rev. Lett. **94**(22), 223902 (2005).
5. H. Rokhsari, T. J. Kippenberg, T. Carmon, and K. J. Vahala, "Radiation-pressure-driven micro-mechanical oscillator," Opt. Express **13**(14), 5293–5301 (2005), http://www.opticsinfobase.org/oe/abstract.cfm?URI=oe-13-14-5293.
6. T. J. Kippenberg, H. Rokhsari, T. Carmon, A. Scherer, and K. J. Vahala, "Analysis of radiation pressure induced mechanical oscillation of an optical microcavity," Phys. Rev. Lett. **95**(3), 033901 (2005).
7. S. Gigan, H. R. Böhm, M. Paternostro, F. Blaser, G. Langer, J. B. Hertzberg, K. C. Schwab, D. Bäuerle, M. Aspelmeyer, and A. Zeilinger, "Self-cooling of a micromirror by radiation pressure," Nature **444**(7115), 67–70 (2006).
8. O. Arcizet, P. F. Cohadon, T. Briant, M. Pinard, and A. Heidmann, "Radiation-pressure cooling and optomechanical instability of a micromirror," Nature **444**(7115), 71–74 (2006).
9. D. Kleckner, and D. Bouwmeester, "Sub-kelvin optical cooling of a micromechanical resonator," Nature **444**(7115), 75–78 (2006).
10. A. Schliesser, P. Del'Haye, N. Nooshi, K. J. Vahala, and T. J. Kippenberg, "Radiation pressure cooling of a micromechanical oscillator using dynamical backaction," Phys. Rev. Lett. **97**(24), 243905 (2006).
11. T. Corbitt, Y. Chen, E. Innerhofer, H. Müller-Ebhardt, D. Ottaway, H. Rehbein, D. Sigg, S. Whitcomb, C. Wipf, and N. Mavalvala, "An all-optical trap for a gram-scale mirror," Phys. Rev. Lett. **98**(15), 150802 (2007).
12. T. Carmon, and K. J. Vahala, "Modal spectroscopy of optoexcited vibrations of a micron-scale on-chip resonator at greater than 1 GHz frequency," Phys. Rev. Lett. **98**(12), 123901 (2007).
13. J. D. Thompson, B. M. Zwickl, A. M. Jayich, F. Marquardt, S. M. Girvin, and J. G. E. Harris, "Strong dispersive coupling of a high-finesse cavity to a micromechanical membrane," Nature **452**(7183), 72–75 (2008).
14. V. B. Braginsky, Measurement of Weak Forces in Physics Experiments (University of Chicago Press, Chicago, 1977).
15. M. L. Povinelli, M. Loncar, M. Ibanescu, E. J. Smythe, S. G. Johnson, F. Capasso, and J. D. Joannopoulos, "Evanescent-wave bonding between optical waveguides," Opt. Lett. **30**(22), 3042–3044 (2005).
16. M. L. Povinelli, S. G. Johnson, M. Loncar, M. Ibanescu, E. J. Smythe, F. Capasso, and J. D. Joannopoulos, "High-Q enhancement of attractive and repulsive optical forces between coupled whispering-gallery- mode resonators," Opt. Express **13**(20), 8286–8295 (2005), http://www.opticsinfobase.org/oe/abstract.cfm?URI=oe-13-20-8286.
17. P. T. Rakich, M. A. Popovic, M. Soljacic, and E. P. Ippen, "Trapping, corralling and spectral bonding of optical resonances through optically induced potentials," Nat. Photonics **1**(11), 658–665 (2007).

#115740 - $15.00 USD Received 14 Aug 2009; revised 26 Sep 2009; accepted 12 Oct 2009; published 30 Oct 2009

18. M. Notomi, H. Taniyama, S. Mitsugi, and E. Kuramochi, "Optomechanical Wavelength and Energy Conversion in High-Q Double-Layer Cavities of Photonic Cystal Slabs," Phys. Rev. Lett. **97**(2), 023903 (2006).
19. M. Eichenfield, C. P. Michael, R. Perahia, and O. Painter, "Actuation of micro-optomechanical systems via cavity-enhanced optical dipole forces," Nat. Photonics **1**(7), 416–422 (2007).
20. M. Li, W. H. P. Pernice, C. Xiong, T. Baehr-Jones, M. Hochberg, and H. X. Tang, "Harnessing optical forces in integrated photonic circuits," Nature **456**(7221), 480–484 (2008).
21. M. Eichenfield, R. Camacho, J. Chan, K. J. Vahala, and O. Painter, "A picogram- and nanometre-scale photonic-crystal optomechanical cavity," Nature **459**(7246), 550–555 (2009).
22. G. Anetsberger, O. Arcizet, Q. P. Unterreithmeier, E. M. Weig, J. P. Kotthaus, and T. J. Kippenberg, "Near-field cavity optomechanics with nanomechanical oscillators," arXiv: 0904.4051v1.
23. Q. Lin, J. Rosenberg, X. Jiang, K. J. Vahala, and O. Painter, "Mechanical oscillation and cooling actuated by the optical gradient force," Phys. Rev. Lett. **103**, 103601 (2009). See also arXiv:0905.2716v1.
24. J. Rosenberg, Q. Lin, and O. Painter, "Static and dynamic wavelength routing via the gradient optical force," Nat. Photonics **3**(8), 478–483 (2009).
25. T. J. Kippenberg, S. M. Spillane, D. K. Armani, and K. J. Vahala, "Fabrication and coupling to planar high-Q silica disk microcavities," Appl. Phys. Lett. **83**(4), 797–799 (2003).
26. T. J. Kippenberg, J. Kalkman, A. Polman, and K. J. Vahala, "Demonstration of an erbium-doped microdisk laser on a silicon chip," Phys. Rev. A **74**(5), 051802 (2006).
27. D. K. Armani, T. J. Kippenberg, S. M. Spillane, and K. J. Vahala, "Ultra-high-Q toroid microcavity on a chip," Nature **421**(6926), 925–928 (2003).
28. M. Cai, O. Painter, and K. J. Vahala, "Observation of critical coupling in a fiber taper to a silica-microsphere whispering-gallery mode system," Phys. Rev. Lett. **85**(1), 74–77 (2000).
29. S. M. Spillane, T. J. Kippenberg, O. J. Painter, and K. J. Vahala, "Ideality in a fiber-taper-coupled microresonator system for application to cavity quantum electrodynamics," Phys. Rev. Lett. **91**(4), 043902 (2003).

1. Introduction

Recently, the coupling of optical cavity modes and mechanical degrees of freedom via radiation pressure is receiving considerable attention [1–3]. Both fundamental and applied studies are driving interest across a wide range of experimental platforms [4–13]. In these devices, the optical scattering force sets up conditions necessary for observation of dynamic backaction [14], enabling both amplification and cooling of mechanical modes. Besides this scattering force, the spatial variation of an intensity distribution can give rise to a gradient or dipole force which has been proposed in coupled optical waveguides [15], microspheres [16], microrings [17] and photonic crystal cavities [18], and has been experimentally demonstrated in integrated photonic circuits [19–24].

Here we describe the design and fabrication of a double-disk microcavity for cavity optomechanics. The structure features a gradient-force-induced optomechanical coupling that enables improved optimization of coupling strength without adversely impacting other device properties. It also supports high optical quality factor whispering-gallery modes, provides for easy fabrication, and low thermo-optic effects. Beyond cavity optomechanics, this structure may also find applications in various fields such as cavity QED, biosensing, optomechanically tuned filters [24], and optical wavelength conversion [18].

#115740 - $15.00 USD Received 14 Aug 2009; revised 26 Sep 2009; accepted 12 Oct 2009; published 30 Oct 2009

2. Optical design and simulation

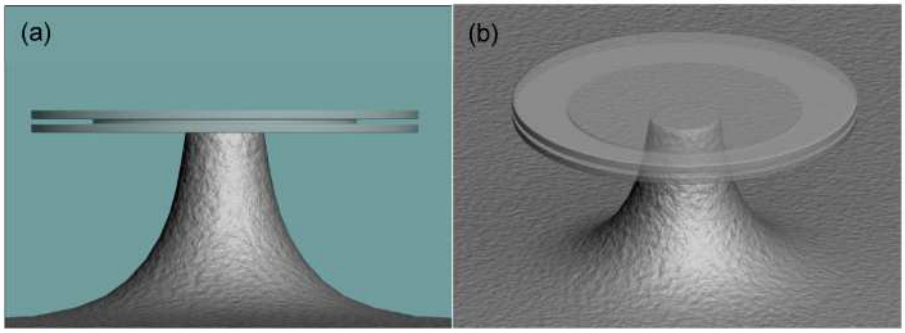

Fig. 1. Schematics of double-disk microcavity.

The double-disk microcavity is illustrated in Fig. 1, and consists of a pair of silica microdisks stacked on top of each other and separated by a nanoscale gap. Using silica as the disk material provides several benefits. First, the negligible optical loss in the silica material helps to support the extremely high optical quality factor of the microcavity, as has been shown in microdisks [25, 26] and microtoroids [27]. Second, its moderate refractive index provides sufficient mode confinement while also allowing the optical mode to spread out from each single disk, thereby enabling strong mode coupling even with a modest disk spacing. Third, silica has a high thermal resistance, significantly reducing the magnitude of possible thermal-optic and thermal-mechanical effects relative to the optomechanical effects [23, 24]. Finally, the amorphous nature of silica glass allows for flexible processing during device fabrication, which will be discussed in detail later.

Well separated disks would feature whispering gallery modes on a spectral grid determined by the disk radius. In the coupled, double-disk geometry, two degenerate (or nearly degenerate) whispering gallery modes will couple evanescently, forming hybridized supermodes that are symmetric and anti-symmetric combinations of the original, uncoupled modes. The gradient force causes attraction of the disks when the symmetric mode is excited, and repulsion for the antisymmetric mode. As a result, these modes can also be called bonding and anti-bonding supermodes in analogy to a chemical bond. Mode profiles are shown in Fig. 2. The required level of degeneracy for the original, uncoupled modes is, in fact, easy to satisfy on account of the strong coupling of the modes. For example, given a 200 nm gap between two 400 nm thick silica microdisks a mode splitting of more than 24 THz occurs between the bonding and anti-bonding modes. This splitting is so large that even modes that are mismatched in frequency by several free-spectral-ranges will nonetheless experience strong coupling and setup the symmetric and anti-symmetric supermode states. This is particularly important as the actual double-disk structure (see Fig. 2(c), 2(d)) features disks that are distinctly different in diameter on account of side-wall etching that is angled. The dependence of bonding mode resonance on gap is plotted in Fig. 3(a).

#115740 - $15.00 USD Received 14 Aug 2009; revised 26 Sep 2009; accepted 12 Oct 2009; published 30 Oct 2009

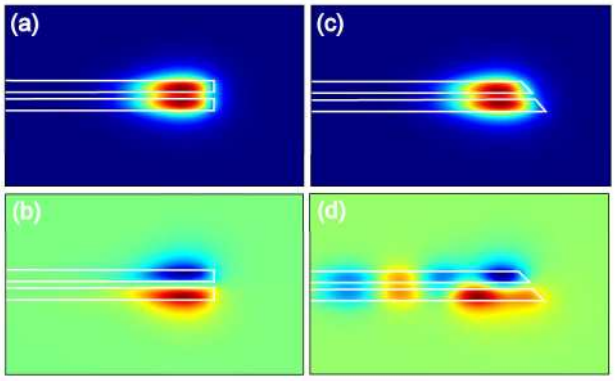

Fig. 2. Mode profiles of the radial component of the electric field for the TE-like cavity mode in a double-disk cavity. (a) bonding and (b) antibonding mode in a cavity with a vertical sidewall. (c) bonding and (d) anti-bonding mode in a practical cavity with a angled sidewall. The mode hybridization is clearly visible for the anti-bonding mode.

The optical gradient force between the two disks can be characterized through the cavity dispersion as $F = -N\hbar g_{OM}$, where N is the total photon number inside the cavity, $\hbar$ is the reduced Plank's constant, and $g_{OM} = d\omega/dx$ is the optomechanical coupling coefficient characterizing the magnitude of the per-photon force. Figure 3(b) shows the optomechanical coupling coefficient versus gap in a double-disk structure with a diameter of 90 μm and a thickness of 400 nm for each disk. It is shown clearly that, with a disk spacing of 200 nm, the optomechanical coupling coefficient can be as large as $2\pi\times27$ GHz/nm. This value is about one order of magnitude higher than other cavities such as Fabry-Perot cavities and microtoroids, showing the extremely strong gradient force provided by the double-disk structure. More importantly, as the mode coupling is primarily determined by the lateral mode confinement, the per-photon force in the double disk is independent of cavity optical-path-length (i.e., disk radius) [23, 24]. This is in strong contrast to other optomechanical cavities, in which the per-photon force scales inversely with the cavity size. For example, in Fabry-Perot cavities g_{OM} scales inversely with cavity length ($g_{OM} = -\omega/L$), and in microtoroids it scales inversely with radius ($g_{OM} = -\omega/R$). Therefore, using double-disks it is possible to realize diverse disk geometries (large or small) while maintaining the same optomechanical coupling strength [24].

#115740 - $15.00 USD Received 14 Aug 2009; revised 26 Sep 2009; accepted 12 Oct 2009; published 30 Oct 2009

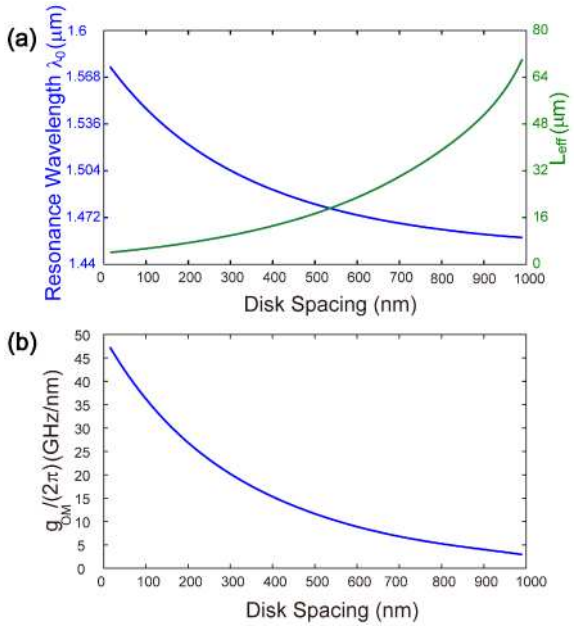

Fig. 3. (a) Resonance wavelength (blue) and effective length (green) as a function of disk spacing, for a TE-like bonding mode. (b) The corresponding optomechanical coupling coefficient.

For easy comparison to other structures, we introduce an effective length L_{eff} defined by $g_{OM}= d\omega/dx = \omega/L_{eff}$ to characterize the gradient force in the double-disk structure [23]. This effective length is given by $L_{eff} = \omega/(d\omega/dx)$. The green curve in Fig. 3(a) shows the effective length as a function of gap for the bonding mode in a 90-μm-diameter microcavity with 400nm thickness silica disks. The effective length increases exponentially with the distance of the two disks. In principle, the minimum effective length can be as small as 4 μm: much smaller than in Fabry-Perot cavities or microtoroids. This value is achievable in practice since current fabrication technique allows the disk spacing to be as small as tens of nanometers.

Note that, in addition to the in-plane TE-like cavity modes presented in Fig. 2, the same device structure also supports orthogonal TM-like mode families. Figure 4 shows a typical mode profile of the TM-like bonding mode. Clearly, due to the distinctive boundary condition of the electromagnetic fields, the optical energy is more confined inside the gap region for the TM-like modes compared with the TE-like modes. This feature is similar to that in a slot waveguide [15]. As a result, the TM-like cavity mode is more sensitive to variations in disk spacing, leading to a stronger optomechanical coupling [24]. As shown clearly in Fig. 4, the optomechanical coupling coefficient in the TM-like mode is about 30-60% higher than that of the TE-like mode [24].

#115740 - $15.00 USD Received 14 Aug 2009; revised 26 Sep 2009; accepted 12 Oct 2009; published 30 Oct 2009

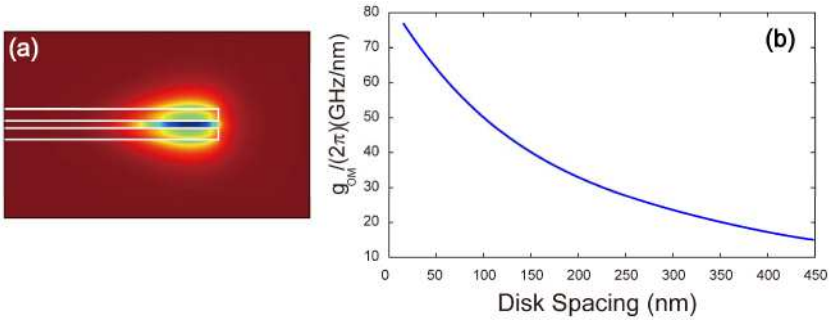

Fig. 4. (a) Mode profiles of the vertical component of the electric field for the TM-like cavity mode. (b) The optomechanical coupling coefficient g_{OM} as a function of disk spacing for the TM-like mode.

Although various optomechanical photonic structures have been proposed and demonstrated to utilize the optical gradient force, in general, these structures exhibit either quite low optical quality factors or a small optomechanical coupling due to either their intrinsic geometric limitations or practical difficulties in device fabrication. As a result, these photonic structures generally has a dynamic backaction efficiency even lower than in conventional optomechanical cavities based on radiation pressure. In contrast, the whispering-gallery nature of the double-disk microcavity described here allows for extremely high quality optical modes circulating around the disk perimeter. In practice, the optical Q factor is primarily limited by the sidewall roughness. However, it can be significantly mitigated by applying a tilted angle to push the optical mode away from the disk perimeter region [26]. FEM simulations show (Fig. 2) that the bonding mode profile remains nearly unchanged with the addition of this sidewall angle. However, the anti-bonding mode experiences significant mode hybridization with higher-order TM-like modes, leading to very low cavity Q factors. As a result, in practice, for devices with very small disk spacing ~100nm, the bonding mode is much easier to observe than the anti-bonding mode [23, 24].

3. Mechanical mode analysis

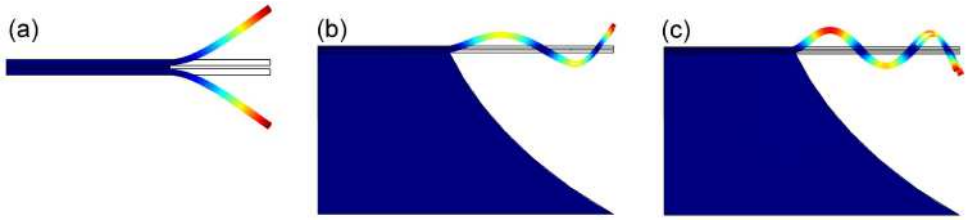

Fig. 5. FEM simulations of three typical mechanical modes in a 90-μm-diameter, double-disk cavity with 7 μm undercut, 400 nm thickness for each disk and 200 nm disk spacing. The color map shows the vertical displacement, exaggerated for clarity.

The double-disk structure supports multiple mechanical normal motions. Some typical examples are shown in Fig. 5, obtained from mechanical FEM simulations. Figure 5(a) shows a lateral flapping mode in which the two disks move opposite to each other. Other modes are radial breathing modes with the two disks moving in parallel. It is clear that only the lateral flapping motion would be strongly actuated by the optical gradient force. In general, the frequency of the flapping mode is dominantly controlled by the length of undercut, while the frequencies of the radial breathing modes are primarily determined by the radius of the pedestal. Due to the whispering-gallery nature of the cavity, the optical mode is pushed to the disk edge and thus is relatively insensitive to the undercut length. This provides flexibility for nearly independent control of the mechanical and optical properties of the structure. By varying the undercut length, we are able to freely engineer the mechanical frequency of the

#115740 - $15.00 USD Received 14 Aug 2009; revised 26 Sep 2009; accepted 12 Oct 2009; published 30 Oct 2009

flapping mode. Figure 6 shows the mechanical frequency as a function of undercut, showing clearly the free control of the mechanical frequency [23, 24].

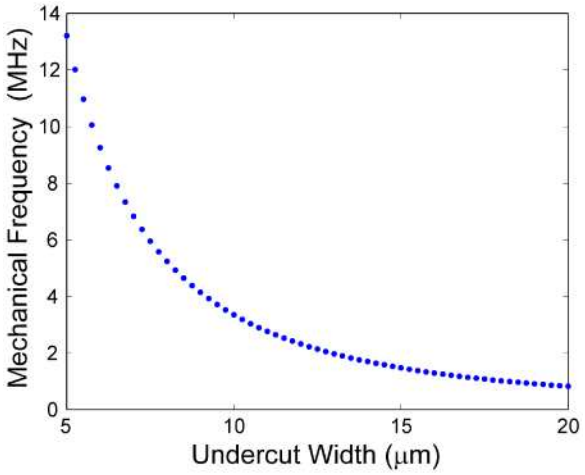

Fig. 6. The mechanical frequency of the flapping mode as a function of undercut width.

The whispering-gallery nature of the structure pushes the cavity mode towards the disk edge, and thus maximizes the mechanical torque for the flapping mechanical motion. Moreover, as the gradient force is symmetric on the two disks, only the undercut regions are involved in the flapping motion. As a result, the flapping mode has a very small effective motional mass [23, 24]. For the example shown in Fig. 5(a), the effective mass is only 334 pg (see Ref [23]. for details about the definition of effective mass), implying a significantly enhanced efficiency of the dynamic backaction. In addition to the undercut length, the effective motional mass also scales inversely with the disk diameter. As a result, by varying the disk diameter while maintaining the same undercut length, we can freely engineer the effective mass without affecting the mechanical frequency [23]. Clearly, the double-disk geometry provides great freedom to independently engineer various aspects of the optomechanical properties of the device, enabling optimization of the structure for diverse applications [23, 24]. In practice, the mechanical quality is primarily determined by the squeeze-film damping from the surrounding gas and the clamping loss from the sandwiched silicon layer [23, 24].

4. Device fabrication

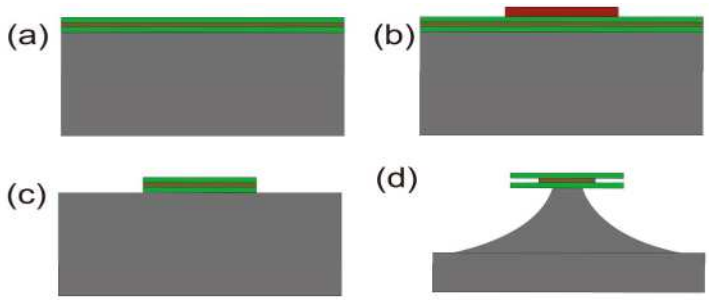

Fig. 7. Schematic description of the procedure for fabricating the double-disk microcavities. (a) Deposition of silica, α-silicon, and silica layers on top of a silicon wafer. (b) E-beam lithography to form the microdisk pattern on the mask. (c) RIE dry etching to produce double microdisks. (d) Plasma dry release to partially remove the silicon layers to form the silicon pedestal and partially undercut sandwiched α-silicon layer.

#115740 - $15.00 USD Received 14 Aug 2009; revised 26 Sep 2009; accepted 12 Oct 2009; published 30 Oct 2009

The main fabrication process for the double disk structure is illustrated in Fig. 7. First, two layers of silica and the sandwiched amorphous silicon (α-Si) layer were deposited on a silicon wafer using plasma-enhanced chemical vapor deposition (PECVD). The wafer was then thermally annealed at 1050 °C for 6 hours under a nitrogen atmosphere in order to densify the PECVD films and improve their optical quality. The double-disk structures were then patterned using electron beam lithography and etched via an anisotropic inductively-coupled plasma reactive ion etch with a C4F8/SF6 gas chemistry. For the final step, the sandwiched α-si layer and the silicon pedestal were simultaneously undercut using a SF_6 chemical plasma release. Figure 8 shows a scanning electron microscope image of the fabricated double disk microcavity.

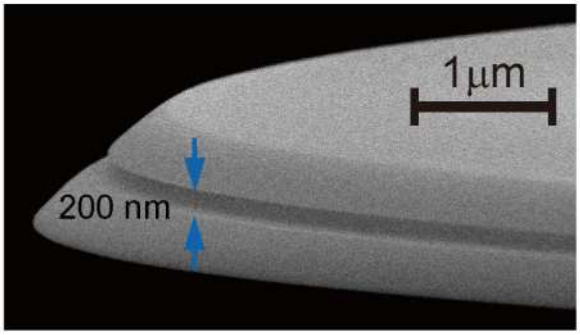

Fig. 8. Scanning electron microscope image of the double-disk edge.

5. Optical mode characterization

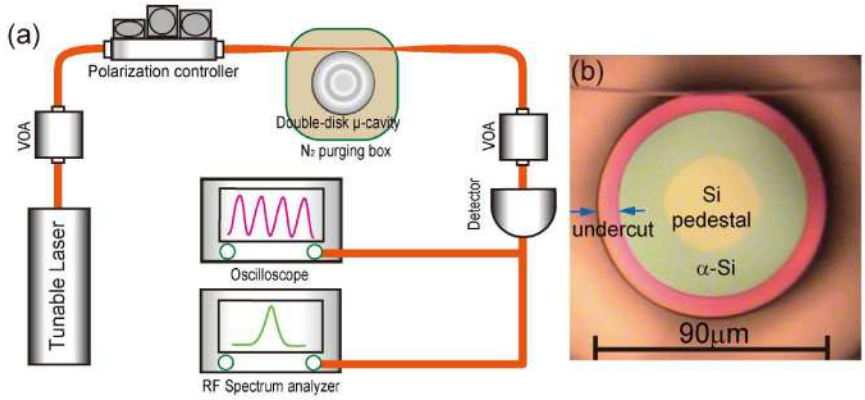

Fig. 9. (a) Schematic of the experimental setup for optical and mechanical measurement. (b) Top-view optical image of the taper-disk coupling system. It is enclosed in a nitrogen environment at atmospheric pressure. VOA: variable optical attenuator.

Figure 9(a) shows the experimental setup used to characterize the fabricated device. A continuous-wave tunable laser is launched into the cavity through a single-mode tapered fiber (Fig. 9(b)) [23, 24, 28, 29]. The cavity output is then measured by a fast detector. Figure 10 shows a typical linear transmission spectrum of a TE-polarized bonding mode in a 90-μm-diameter double-disk microcavity. The input optical power is maintained at a very low level (2.8 μW) to prevent any thermal nonlinearity. The measured free spectral range (FSR) is ~6 nm. A detailed scan (inset of Fig. 10(a)) of the bonding mode at a wavelength of 1512.80 nm indicates an intrinsic quality factor of about 1 million. The optical Q factor is primarily limited by the sidewall roughness, the structure uniformity, and the optical quality of the

#115740 - $15.00 USD Received 14 Aug 2009; revised 26 Sep 2009; accepted 12 Oct 2009; published 30 Oct 2009

PECVD material. As discussed previously, the high mode hybridization prevents observation of the anti-bonding mode in this spectral region.

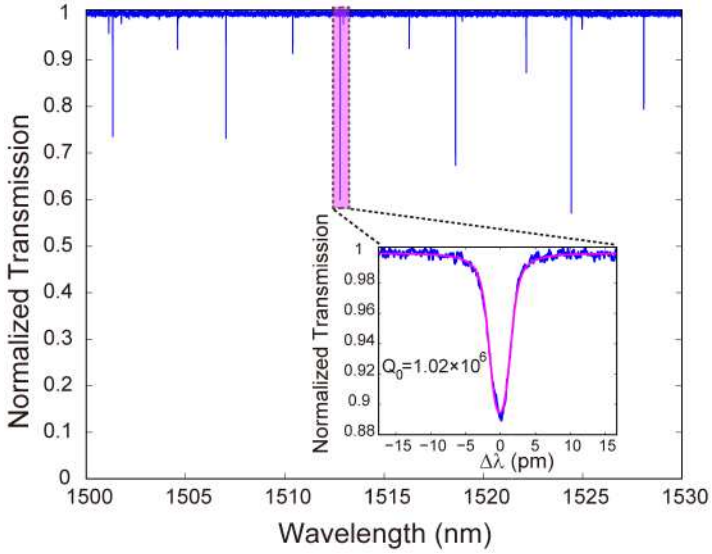

Fig. 10. Linear scan of cavity transmission. The inset shows a detailed scan of the bonding mode at 1512.80 nm, with experimental data in blue and theoretical fit in red.

6. Conclusion

In conclusion, we have described and demonstrated a double-disk structure for cavity optomechanics. Both optical and mechanical analyses have been discussed. The mechanical frequency of the flapping mode can be tuned by controlling the undercut of the sandwiched α-Si layer without affecting the optical mode of the cavity. In addition, we have demonstrated the fabrication of a double-disk microcavity with a quality factor of about 1 million. Beyond cavity optomechanics, we believe that the double-disk structure can also find applications in various fields such as biosensing, tunable filtering [24], and optical wavelength conversion [18].

Acknowledgments

This work was supported by DARPA. Xiaoshun Jiang is also grateful for the support of the China Scholarship Council.

#115740 - $15.00 USD Received 14 Aug 2009; revised 26 Sep 2009; accepted 12 Oct 2009; published 30 Oct 2009